Guanylate binding protein 2b contributes to M1 macrophage polarization during Mycobacterium bovis infection

Youli Yu
Nanjing Agricultural University
Mengting Liu
Nanjing Agricultural University
Jialiang Pan
Nanjing Agricultural University
Lei Tao
Nanjing Institute for Food and Drug Control
Feng Xue (xuefeng@njau.edu.cn)
Nanjing Agricultural University
Fang Tang
Nanjing Agricultural University
Hongsheng Wang
Chinese Academy of Medical Sciences and Peking Union Medical College
Jianjun Dai
China Pharmaceutical University
Yuping Shan
Lianyungang Animal Husbandry and Veterinary Station

Research Article

Keywords: Mycobacterium bovis, GBP2b, M1 polarization, Antibacterial, TLR-4/NF-κBp65 pathway

Posted Date: May 16th, 2022

DOI: https://doi.org/10.21203/rs.3.rs-1631961/v1

Abstract

Accumulating evidence has demonstrated that the macrophage phenotype switch from M0 to M1 is critical in the clearance of intracellular mycobacteria during *Mycobacterium bovis* infection. In this study, the entire gene expression profiles of M1 bone marrow-derived macrophages (BMDMs) induced by interferon-gamma and lipopolysaccharide, M2 BMDMs induced by interleukin (IL) - 4 and IL-13, M0 BMDMs, and M0 BMDMs after 6 h of infection with *M. bovis* were subjected to bioinformatics analysis. Forty-eight candidate genes associated with *M. bovis* infection and involved in M1 polarized macrophages were screened. Thirteen hub genes were subsequently identified based on connectivity degree analysis and multiple external validations. Among these hub genes, Guanylate binding protein 2b (GBP2b) was selected as a key gene for further investigation. In vivo validation results showed significant expression of GBP2b in the tissues of *M. bovis* -infected mice. For in vitro validation, the RAW264.7 cell line was transfected with GBP2b-specific small interfering RNA and GBP2b plasmid expression vector. Cellular experimental studies confirm that GBP2b was a novel regulatory molecule that promotes M1 macrophage polarization during *M. bovis* infection and was also an antimicrobial protein that promotes intracellular bacterial clearance. Furthermore, gene co-expression analysis and further experiments showed that GBP2b regulates M1 polarization through activation of Toll-like receptor 4 and nuclear factor-κBp65 protein. These findings expand the understanding of GBP2b for the regulation of inflammatory responses and suggest that GBP2b may be a potential target for the treatment of diseases caused by *M. bovis.*

Introduction

Mycobacterium bovis belongs to the *Mycobacterium tuberculosis* complex and is the main pathogen causing bovine tuberculosis. In turn, this pathogen is also a common cause of human tuberculosis [1]. Although human and animal tuberculosis caused by *M. bovis* is relatively rare in developed countries, it is still a serious problem in less developed regions. Some reports indicate that the risk of *M. bovis* is underestimated. Cure rates are comparable in patients with *M. bovis* and *M. tuberculosis*, but death is more frequent in patients with *M. bovis* than in those with *M. tuberculosis* [1, 2]. Therefore, elucidating the different mechanisms of host defense against *M. bovis* infection is important.

Macrophages, as the primary effector cells in response to *M. bovis* infection, are highly plastic [2]. In response to various stimuli, macrophages can be divided into M1 (classically activated macrophages) and M2 (alternatively activated macrophages) phenotypes [3]. Under the stimulation of interferon-γ (IFN-γ) and lipopolysaccharide (LPS), the initial state of macrophages (M0) can differentiate into M1-like macrophages, which secrete a large number of pro-inflammatory and chemotactic factor, has the strong bactericidal ability. By contrast, M2-like macrophages induced by interleukin (IL) -4 and IL-13 produce small amounts of inflammatory cytokines (eg, IL-10 and IL-12), promote tissue remodeling and repair, and exhibit low antigen-presenting capacity[4]. Existing studies on macrophage polarization have identified some of the molecules and signaling pathways associated with M1 polarization. However, these studies

mostly focused on tumors and other disease studies rather than on diseases caused by *M. bovis*. The molecular mechanisms involved in macrophage polarization in *M. bovis* infection remain unclear.

Guanylate-binding protein 1 (GBP1/GBP2b) is a member of the large family of IFN-γ-inducible GTPases. GBP2b is widely involved in the regulation of various cellular functions, including the regulation of processes such as pyroptosis, polarization, apoptosis, and autophagy [5–7]. Studies have shown that GBP2b directly binds to cytosolic LPS, bringing the inflammatory cysteine caspase 4 to the bacterial surface to induce pyroptosis [5]. During inflammatory psoriasis, GBP2b promotes the differentiation of IFN-γ-driven human monocytes into highly pro-inflammatory macrophages [8]. In addition, bioinformatic analysis of all gene expression profiles of patients with acute respiratory distress syndrome revealed that GBP2b is a pivotal gene promoting M1 macrophage polarization [9]. Another study combined proteomics with co-abundance network analysis and predicted GBP2b as a novel candidate protein for promoting macrophage inflammation [10]. These findings reveal that GBP2b has an important regulatory function in macrophage inflammation and plays a role in macrophage polarization. However, the function of GBP2b during *M. bovis* infection is unknown.

In this study, the differentially expressed gene GBP2b was identified as a key regulatory molecule that may be simultaneously involved in *M. bovis* infection and M1 macrophage polarization by using bioinformatic analysis and experiments. Furthermore, GBP2b knockdown and overexpression transfected RAW264.7 cell lines were constructed to confirm that GBP2b is a novel molecular regulator of M1 macrophage polarization. The subsequent bioinformatic analysis and biological pathway experiments showed that GBP2b regulates M1 macrophage polarization through the TLR4/NF-κBp65 pathway.

Results

Differential genes associated with *M. bovis* infection and M1-polarized macrophages

To screen for genes that may be involved in macrophage polarization, we induced M0 BMDMs to become M1 BMDMs or M2 BMDMs, respectively. Subsequently, we analyzed differentially expressed genes in M1 BMDMs compared with M0 BMDMs (BMDMs without cytokine induction) or M1 BMDMs compared with M2 BMDMs (p-value < 0.05, log2 FC > 1). The analysis yielded 2088 differential genes in M1 BMDMs compared with M0 BMDMs, including 611 upregulated genes and 1477 downregulated genes (Fig. 1a; Table S1). M1 BMDMs had 2459 differential genes when compared to M2 BMDMs, including 1043 upregulated genes and 1416 downregulated genes (Fig. 1b; Table S2). To further screen for genes associated with *M. bovis* infection in macrophages, we analyzed the gene expression profiles of M0 BMDMs after 6 h of *M. bovis* infection and uninfected M0 BMDMs. The clustering heat map shows 2353 differential mRNAs, (p-value < 0.05 and log2 FC>1) of which 1109 were upregulated and 1244 were downregulated (Fig. 1c; Table S3). These differential genes are mainly enriched in cytokine - cytokine receptor interaction, TNF signaling pathway, NF-kappa B signaling pathway, NOD-like receptor signaling pathway, Toll-like receptor signaling pathway, and MAPK signaling pathway (Fig.1d, e; Table S4).

A Venn diagram was drawn to capture the overlap genes between different comparison groups and 48 candidate genes were screened for *M. bovis* infection and M1 macrophage polarization (Fig. 2a; Table S5).

GBP2b was identified as a key candidate for further investigation

To identify hub genes among the 48 candidate genes, we mapped the mRNA-Co-expression-Network showing up-or down-regulated core genes and calculated the total number of connections (number of interactions) for each node in the network through connectivity degree analysis (Fig. 2b, C; Table S6). As shown in Fig 2c, 13 genes such as IL-6, Ccl5, Cxcl9, Ccrl2, Lcn2, Cd40, Nos2, Serpina3g, Ccr2, Saa3, GBP2b, ligp1, and Il1a have more than 15 junctions. Thus, these genes are considered to be hub genes associated with *M. bovis* infection and M1 macrophage polarization.

To further validate the expression levels of the 13 hub genes in M0, M1, M2 BMDMs, and M0 BMDMs infected with *M. bovis* for 6 h, we examined the mRNA levels of these 13 hubs genes through qRT-PCR (Fig. S1a, b). The expression levels of these 13 hub genes were consistent with the RNA-Seq data, thus demonstrating the high confidence of RNA-Seq analysis. Among these hub genes, GBP2b was targeted for further study. Several research reports that GBP2b, an antimicrobial protein, maybe a key gene in promoting inflammatory response and M1 macrophage polarization,but the exact mechanism is unclear [11, 12].

First, we examined the expression of GBP2b in BMDMs and RAW264.7 cells under different polarization states. The results demonstrated that the protein and mRNA levels of GBP2b were highest in M1 macrophages and lowest in M2 macrophages in both cells (Fig. 2d, e). We next examined the expression of GBP2b during *M. bovis* infection. Western blot results demonstrated that *M. bovis* infection elevated the expression of GBP2b in BMDMs and RAW264.7 cells at different time points (6, 12, and 24h) compared to the uninfected group (0 h; Fig. 2f, g). The results of in vivo infection experiments demonstrated that the protein and mRNA levels of GBP2b were significantly elevated in the lungs and spleens of mice infected with *M. bovis* for 6 weeks compared with the PBS group (Fig. 2h, i). These results suggest that GBP2b is associated with *M. bovis* infection and M1 macrophage polarization.

GBP2b regulates the balance of *M. bovis* replication in macrophages

Mice knocked out of GBP2b are more likely to die from BCG infection, demonstrating that GBP2b contributes to host resistance to BCG (12). However, whether or not GBP2b is equally effective against the strong virulent strain *M. bovis* has not been reported. Therefore, in the present study, we quantified intracellular bacterial CFU by silencing or overexpressing GBP2b in RAW264.7 cells after subsequent infection with *M. bovis* at different time points (6, 12, 24, and 48 h). Silencing GBP2b significantly increased bacterial CFU in RAW264.7 cells, especially at 24 h post-infection (Fig. 3a). By contrast, upregulation of GBP2b expression downregulated bacterial CFU within RAW264.7 cells (Fig. 3b). These results suggest that GBP2b exerts antibacterial effects during *M. bovis* infection and enhances the bactericidal activity of macrophages.

M. bovis infection induces macrophage polarization toward M1

Macrophages can be polarized into a pro-inflammatory cell population (M1-like macrophages) at any time point of *M. bovis* infection, especially early in the infection (10). M1 macrophages secrete inflammatory cytokines and chemokines to further activate and recruit immune cells, thereby contributing to the sustained killing and clearance of intracellular mycobacteria by the host cells [13]. Therefore, the polarization of macrophages to the M1 phenotype during *M. bovis* infection may be of therapeutic value. First, we examined the macrophage polarization after *M. bovis* infection with BMDMs and RAW264.7 cells at different times. Western blot results demonstrated that M1 markers such as inducible NO synthase (iNOS) and tumor necrosis factor-α (TNF-a) protein levels were upregulated at different time points (0, 6, 12, and 24 h) after *M. bovis* infection compared to the uninfected group (Fig. 4a, b). Flow cytometry results of the proportion of CD86-labeled cells (M1 macrophages marker) showed that compared to the uninfected group, the proportion of CD86 cells was upregulated at different time points (0, 6, 12, and 24 h) after *M. bovis* infection (Fig. 4c, d). These results suggest that infection of macrophages by *M. bovis* regulates macrophage polarization toward M1.

GBP2b promotes the polarization of *M. bovis*-infected macrophages toward M1

To verify whether GBP2b is a key gene in promoting M1 macrophage polarization and inflammatory response during *M. bovis* infection, we introduced siRNA sequences and GBP2b plasmid expression vector to transfect RAW264.7 cells to silence or overexpress the GBP2b. As shown in Fig S2 (S2a, c), siRNA sequences and plasmid expression vectors were able to silence and overexpress GBP2b in RAW264.7 cells, respectively. The results of qPCR and Western blot revealed that mRNA levels of M1 macrophage markers (e.g., iNOS, TNF-a, IL-1β, and IL-6) and protein levels of iNOS and TNF-a were down-regulated in RAW264.7 cells silenced with GBP2b and infected with *M. bovis* for 24h, compared with the control group. (Fig. 5a, c). The opposite result was observed in RAW264.7 cell overexpression of GBP2b, especially in the infected group (Fig. 5b, d).

In addition, we examined other M1 macrophage markers. Flow cytometry results of the proportion of CD86-labeled cells following silencing of GBP2b in RAW264.7 cells and then infected with *M. bovis* for 24 h revealed that silencing of GBP2b downregulated the proportion of CD86-labeled cells compared to the control group (Fig. 5e). The opposite result was observed for GBP2b overexpression, especially more significant in the infected group (Fig. 5f). The above results support that GBP2b is a regulatory molecule that promotes the M1 macrophage polarization during *M. bovis* infection.

GBP2b promotes NO and ROS release during *M.bovis* infection

NO, and ROS are the powerful antibacterial mechanism for host cell defense against intracellular mycobacteria and also serves as a marker of M1 polarization [14-16]. In the present study, down-regulation of GBP2b significantly reduced NO and ROS release compared with the control group, whereas up-regulation of GBP2b increased NO and ROS release, especially more significantly in the *M. bovis*

infection group (Fig.6 a-d). These results suggest that GBP2b exerts its antimicrobial function by promoting the release of bactericidal mediators during *M. bovis* infection.

GBP2b promotes M1 polarization in macrophages via TLR4/NF-κBp65 signaling during *M. bovis* infection

The above results indicate that GBP2b promotes M1 macrophage polarization during *M. bovis* infection. In the next experiments, we wanted to explore the pathways through which GBP2b is involved in this process. The GBP2b-ComRNA-Pathway-Network was constructed to show the pathways mainly regulated by GBP2b (Table S7, S8). As shown in Fig 7a, the signaling pathways involved in GBP2b include the TNF signaling pathway in regulating apoptosis in Mycobacterium infected host cells; The NF-κB signaling pathway and MAPK signaling pathway are the core signals mediating the inflammatory response; The pathogen pattern recognition receptors Toll-like receptor signaling pathway and NOD-like receptor signaling pathway. Differentially expressed mRNAs and signaling pathways identified here, may all be associated with *M. bovis* infection or host resistance to infection.

TLR signaling pathway plays a major role in the regulation of innate immunity against mycobacterial infection. It activates adaptive immunity by regulating the production of pro-inflammatory factors and chemokines by host cells, and recruits and activates phagocytes to the infection site to clear Mycobacterium [17, 18]. By silencing or overexpressing GBP2b in RAW264.7 cells, we found that GBP2b downregulation decreased TLR4 protein levels compared to the control group, especially after infection (Fig. 7b). By contrast, upregulation of GBP2b increased TLR4 expression (Fig. 7c). In addition, RNAi technology was used to specifically knockdown TLR4 expression in RAW264.7 cells and investigate the effect of TLR4 depletion on GBP2b expression after *M. bovis* infection (Fig. S2b). The results demonstrated that downregulation of TLR4 in RAW264.7 cells exerted no significant effect on the level of GBP2b after *M. bovis* infection compared with the control (Fig. 7c). These data suggest that GBP2b is an upstream molecule that mediates TLR4 expression.

TLR signaling pathway is known to initiate the NF-κB signaling pathway through the MyD88 molecule [19]. Further, NF-κB is activated after IκB degradation and translocated to the nucleus to promote the expression of pro-inflammatory genes. We noticed that downregulation of GBP2b expression and infection with *M. bovis* for 24 h resulted in a downregulation of the phosphorylation level of NF-κBp65 (Fig. 8a) and a significant inhibition of the nuclear translocation of NF-κBp65 compared to the control (Fig. 8c). By contrast, upregulation of GBP2b increased the phosphorylation level of NF-κBp65 (Fig. 8b) and promoted the nuclear translocation of NF-κBp65 (Fig. 8d). This result suggests that GBP2b also exerts a regulatory effect on NF-κBp65 protein. BAY11-7082, a specific inhibitor of NF-κB, could significantly downregulate the protein level of NF-κB but had no significant effect on the expression of GBP2b (Fig. 8e, f). These results suggest that GBP2b is upstream of TLR4/NF-κBp65 signaling and mediates M1 macrophage polarization and inflammatory responses through the TLR4/NF-κBp65 signaling pathway.

Discussion

Tuberculosis (TB) caused by *M. bovis* infection is a chronic inflammatory disease. The ability of *M. bovis* to grow rapidly in host macrophages is an important factor contributing to enhanced bacterial virulence and disease progression. The bactericidal function of phagocytes is strictly dependent on the activation state of the host cell and is regulated by infectious factors and cytokines [16]. During *M. bovis* infection, the conversion of macrophages from the M0 phenotype to the M1 phenotype and the expression of genes with pro-inflammatory mediators are essential to control intracellular *M. bovis* replication (10). Several studies report that the expression of NMAAP1 protein is upregulated in BCG-infected macrophages and that NMAAP1 promotes the polarization of macrophages towards the M1 type, thereby enhancing the phagocytic and bactericidal capacity of macrophages [20]. *M. tuberculosis* PPE36 inhibits macrophage polarization into mature M1 macrophages by inhibiting ERK signaling [21].Knockdown of HMGN2 in macrophages promotes the polarization of macrophages to M1 macrophages during non-tuberculous mycobacterial infection and regulates non-tuberculous mycobacterial survival [22].

Based on the importance of M1-like macrophages in *M. bovis* infection, we performed RNA-sequencing and bioinformatics analysis using macrophages with different activation phenotypes and *M. bovis*-infected macrophages. The differential gene GBP2b associated with *M. bovis* infection and M1 macrophage polarization was screened as a target for further study. Further experiments at the cellular level confirmed that GBP2b exerts an antibacterial function during *M. bovis* infection. More importantly, GBP2b is a novel regulatory molecule that promotes M1 macrophage polarization via the TLR4/NF-κBp65 pathway during *M. bovis* infection. Previous studies on other diseases have shown that GBP2b acts as an upstream regulator of multiple forms of cell death and can promote the activation of microbial-specific downstream pathways involved in the bactericidal process [6, 23]. GBP2b can mediate the release of cytosolic microbial ligands from pathogens and promote innate immune detection, thereby mediating inflammatory responses [24]. In the present study, during *M. bovis* infection, GBP2b upregulates the expression of M1 macrophage markers and regulates the polarization of macrophages towards the M1 phenotype. GBP2b promotes the production of bactericidal mediators NO and ROS, thereby enhancing macrophages' sterilization function. In addition, GBP1 has been established as a powerful marker of inflammation and can be detected in various disease-related inflamed tissues such as psoriasis, lupus erythematosus, adverse drug reactions, and Kaposi's sarcoma, among others [25-27]. These findings also add to the evidence that GBP2b is associated with inflammatory responses.

The innate immune system of the host cell is the most effective defense system against intracellular mycobacteria, in which autoreceptors of macrophages, such as pattern recognition receptors (PRRs), play a key role in recognizing bacteria. Toll-like receptors (TLRs) are major members of the PRR family and play a central role in innate immunity [28]. In the present study, by tracing the signaling pathway regulated by GBP2b, we found that it was involved in regulating the Toll-like receptor signaling pathway and NF-κB signaling pathway. Silencing or overexpression of GBP2b upregulates or downregulates TLR4 expression, respectively. However, TLR4 RNAi knockdown experiments showed that GBP2b was not significantly regulated by TLR4, suggesting that GBP2b may be upstream of

TLR4. Studies on TLR4 downstream signaling NF-κBp65 showed that GBP2b activates NF-kB signaling by upregulating NF-kBp65 phosphorylation levels and promoting significant nuclear translocation of NF-kBp65, which mediates the expression of downstream inflammatory genes. Furthermore, the NF-κBp65 inhibitor Bay11-7082 significantly inhibited the expression of NF-κB p65 but had no significant effect on the expression of GBP2b. These results suggest that GBP2b is an activator of M1 macrophage polarization, TLR4/NF-κB pathway, and signaling of the inflammatory network. Future studies may focus on molecules downstream of the TLR4/NF-κB pathway to explore new GBP2b binding molecules.

Based on these findings, we constructed a model of the potential mechanism by which GBP2b regulates macrophage polarization during *M. bovis* infection. In conclusion, GBP2b is a novel regulatory molecule that promotes M1 macrophage polarization and enhances macrophage bactericidal capacity during *M. bovis* infection. Our study provides new insights into future treatment strategies for TB.

Materials And Methods

Reagents and antibodies

The rabbit anti-GBP1 polyclonal antibody (Catalog No. PA5-23509) was purchased from Life technologies. The following rabbit antibodies, including anti-iNOS (Catalog No. 13120), anti-TNF-a (Catalog No. 11948), anti-NF-κBp65 (Catalog No. 8242) anti-phospho-NF-κBp65 (Catalog No. 3033), anti-β-actin (Catalog No. 8457), anti-TLR4 (Catalog No. 14358), and the goat anti-rabbit secondary antibody (Catalog No. 7074) were purchased from Cell Signaling Technology (Boston, Mass, USA). APC-conjugated anti-mouse CD86 antibody was purchased from R&D Systems (Minneapolis, MN). Nuclear dye DAPI was purchased from Thermo Fisher Scientific (Waltham, MA).

Bacterial culture and infections

Virulent *M. bovis* Beijing strain was obtained from the China Institute of Veterinary Drug Control (CVCC, China). *M. bovis* was cultured in 7H9 Middlebrook media (Catalog No. BD271310, BD Biosciences) containing 10% OADC enhancement solution (Catalog No. BD 212352, BD Biosciences) and incubated continuously for a week at 37 °C to medium logarithmic period. BMDMs and RAW264.7 cells were infected with *M. bovis* (MOI 10) at 37°C with 5% CO2. Cells were washed three times with warm PBS to remove extracellular bacteria after 3 h.

Macrophage culture, induction, and RNA isolation

RAW264.7 cell line (Catalog No. BNCC354753) purchased from ATCC and cultured in Dulbecco's Modified Eagle Medium (Catalog No.10313021, Thermo Fisher Scientific) containing 10% fetal bovine serum (FBS; Catalog No.10099141C, Thermo Fisher Scientific). As described previously [13], BMDMs were isolated from C57BL/6 mice. BMDMs were cultured in Roswell Park Memorial Institutes 1640 Medium containing 20 ng/mL recombinant murine M-CSF (Catalog No. AF-315-02-100, Pepro Tech) and 10% FBS for 5-7

days to become adherent macrophages, and these cells were named M0 BMDMs. Subsequently, M0 BMDM was converted to M1 BMDM after induction by 100 ng/ml LPS and 50 ng/ml IFN-γ for 48 h. M0 BMDM was converted to M2 BMDM after induction by 10 ng/ml IL-4 and IL-13 for 48 h. Four sets of cell samples (M1 BMDMs, M2 BMDMs, M0 BMDMs, and M0 BMDMs infected with *M. bovis* for 6 h) for RNA sequencing, with three biological replicates per sample. RNeasy Mini kit (Catalog No.74104, Qiagen) was used to obtain total RNA with the manufacturer's protocol. RNA samples were quantified and quality controlled with a Nanodrop Lite spectrophotometer (Thermo Fisher Scientific, USA). Finally, RNA samples with a spectral A260/A280 nm ratio between 1.8 and 2.0 and an A260/A230 nm ratio >1.5 were selected for analysis.

Analysis of differentially expressed mRNAs

As previously described [29, 30], the R package DESeq2 algorithm was used to identify differentially expressed genes and mRNAs for identifying transcripts from RNA sequence data. q-value < 0.05 and log2 FC > 1 indicate thresholds for differentially expressed genes.

Pathway analysis

As previously described [29, 30], pathway analysis was performed to identify significant pathways for differential genes based on KEGG. Fisher's exact test and χ2 test were used to select significant pathways, and significance thresholds were determined by *p*-values.

GBP2b-mRNA co-expression correlation analysis

The differential mRNAs associated with GBP2b were screened by calculating the threshold of Pearson |R| > 0.95 between GBP2b and differential mRNAs, and then the pathway regulatory relationships involved in the differential mRNAs were used to establish the GBP2b-ComRNA-Pathway-Network, demonstrating the pathway mainly regulated by GBP2b.

Knockdown of GBP2b and TLR4 expression

Three siRNA sequences specifically targeting mouse GBP2b and mouse TLR4 were designed according to Gene Chem Co., Ltd. (http://www.genechem.com.cn), and siRNA sequences are shown in Table 1. Finally, the efficiency of GBP2b and TLR4 knockdown was examined using RT-PCR and Western blot 48 h after transfection, and the most efficient siGBP2b-3 and siTLR4 -3 were finally determined.

Overexpression of GBP2b

The full-length coding sequence of GBP2b (NM_010259.2, 1800 bp) was amplified by PCR from RAW264.7 cells cRNA, cloned into the pLVX-Puro vector, and then sequenced. The primers for GBP2b are as follows:

XhoI-GBP2b-pF: ATCGCTAGCGCTACCGGACTCAGATctcgagATGGCCTCAGAAATCCACATGAAA

GGCCCAGTGTGC

BamHI-GBP2b-pR:CCGGTAGAATTATCTAGAGTCGCGgatccTTAGTGGTGGTGGT GGTGGTGAAG

TATGGTGCATGATC

The PCR products were purified and cloned into the pLVX-Puro plasmid and then sequenced. The GBP2b overexpression plasmid (pLVX-GBP2b) and an empty vector (pLVX-Con) were transfected into RAW264.7 cells with Lipofectamine 3000 reagent (Catalog No. L3000001, Thermo Fisher Scientific). The protein expression of GBP2b was detected by Western blot to evaluate the overexpression efficiency of transfection.

Quantitative real-time PCR (qRT-PCR)

Total RNA was extracted using the RNeasy Mini kit (Catalog No.74104, Qiagen), and the concentration and integrity were detected by Nanodrop Lite spectrophotometer (Thermo Fisher Scientific, USA). Prime Script TM RT Master Mix (Catalog No. RR036B, Takara) was used for the reverse transcription of RNA to cDNA. RT-PCR analysis was performed using FastStart Universal SYBR Green (Catalog No. 4913850001, Takara) and Light cycler 480 RT-PCR instruments. The results were normalized to GAPDH, and quantification was performed on the $2^{-\Delta\Delta Ct \text{ of each sample}}/2^{-\Delta\Delta Ct \text{ of the Ctrl}}$ method. The primers are listed in Table 2.

Animal and *M. bovis* infection

C57BL/6 mice (male, aged 6–8 weeks) were purchased from Yangzhou University (Yangzhou, China) and raised in a level III biosafety facility (Nanjing Institute for Food and Drug Control, Nanjing). The mice were divided into two groups of 6 mice each. In one group, 200 CFU of *M. bovis* per mouse were given intranasally. The other group was inoculated with the same dose of sterile PBS. After 6 weeks, the spleens and lungs of both groups of mice were collected to detect GBP2b protein and mRNA levels.

Colony-forming unit (CFU)

RAW264.7 cells were transfected with GBP2b silencing vectors (siGBP2b), GBP2b overexpression vectors (pLVX-GBP2b), and the respective negative control vectors (siCon and pLVX-Con) and then infected with *M. bovis* (MOI 10) at different time points. RAW264.7 cells were subsequently washed three times with warm PBS and lysed with sterile 0.2% Triton X100/PBS for 5 min. After serial dilutions of cell lysates, 100 µL of homogenate was evenly spread in a 7H11 solid medium (Catalog No. BD 283810, BD Biosciences) and left at 37 °C for 3-4 weeks. Bacterial CFUs were counted to assess the bactericidal capacity of the cells in the different treatment groups.

Griess assay

The culture supernatant under each culture condition was collected, and the concentration of nitrite in the supernatant was determined using Griess reagent (Catalog No. 13547, Cell Signaling Technology) with the manufacturer's instructions. Finally, the absorbance of the samples was obtained at 540 nm on a microplate reading instrument.

Immunofluorescence

Immunofluorescence analysis was performed to identify the localization of NF-κBp65 in RAW264.7 cells transfected with the GBP2b silencing vector (siGBP2b), the GBP2b overexpression vector (pLVX-GBP2b), and the corresponding negative control vectors (siCon and pLVX-Con) and then infected with *M. bovis* for 24 h. In brief, cells were fixed with 4% paraformaldehyde for 25 min, washed three times with PBS, and then permeabilized for 10 min after containing 0.2% Triton X-100/PBS. Cells were subsequently blocked with 3% bovine serum albumin for 1 h at room temperature, and then anti-NF-κBp65 was incubated overnight at 4 °C. Finally, cells were incubated with Alexa Fluor 647-conjugated anti-rabbit antibody for 1 h, and nuclear staining was performed using DAPI. The cells were visualized immediately with an OLYMPUS microscope (Suzhou Jing Kai Instrument and Equipment Co., Ltd., Suzhou, China). Approximately 100 cells are used to calculate the fluorescence intensity. The Image J software was used for the analysis.

Flow cytometry

BMDMs and RAW264.7 cells from different treatment groups were collected and incubated for 30 min with an APC-conjugated anti-mouse CD86 antibody (1:200) or CellROX reagent (a highly ROS-specific probe, Catalog No. C10488, Thermo Fisher Scientific), respectively. CD86 is used as a marker for M1 macrophages. CellROX is used to detect intracellular ROS. Finally, the cells were resuspended at 500 μL in PBS and FACS caliber flow cytometry (BD, Franklin Lakes, USA). Data were analyzed by Flow Jo software.

Western blot

After different treatments, BMDMs, RAW264.7 cells, mouse lung, and spleen tissues were washed three times with cold PBS and lysed with RIPA buffer (Catalog No. P0013C, Beyotime) containing protease inhibitors. Protein concentration was quantified by a BCA protein analysis kit (Catalog No. P0012S, Beyotime), and protein was transferred to polyvinylidene fluoride membranes (Catalog No.88518, Thermo Fisher Scientific,) following separation on SDS-PAGE gels. The membranes were incubated with primary antibodies overnight at 4 °C and then washed three times with TBST buffer. Subsequently, they were exposed to peroxidase-coupled secondary antibodies for 1 h at room temperature. Finally, the protein bands were visualized with an enhanced chemiluminescence solution. Image J software is used to analyze protein expression and β-Actin acts as load control.

Statistical analysis

The gene expression was calculated by RSEM (v1.2.12) https://github.com/ deweylab/RSEM). The heatmap was drawn by heatmap (v1.0.8) (https://cran.r-project.org/web/packages/pheatmap

/index.html) according to the gene expression in different samples. Essentially, differential expression analysis was performed using the DESeq2 (v1.4.5) (http://www.bioconductor.org/packages/release/bioc/html/DESeq2.html) with a Q value ≤ 0.05. KEGG (https://www.kegg.jp/) enrichment analysis of annotated different expression genes was performed by Pyper (https://en.wikipedia.org/wiki/ Hypergeometric_distribution) based on the Hypergeometric test. GraphPad Prism 8.0.1 was applied to analyze all the experimental data. Data are presented as the means ± standard error or mean ± standard deviation. $P < 0.05$ was considered significant. All assays were performed on at least two or three separate occasions in triplicate each time.

Declarations

Animal ethics statement

All procedures using SPF C57BL/6 mice were approved by the International Society for the Evaluation and Accreditation of Laboratory Animal Management. All animal experiments were approved by the Ethics Committee for Animal Experiments (PTA2019024) of Nanjing Agricultural University, Nanjing, China.

Author Contributions

F.X. and H.S.W. conceived the study; J.L.P. and M.T.L. performed the experiments; F.T., L.T., Y.P.S., and J.J.D. analyzed the experimental results; Y.L.Y. wrote the manuscript. All authors read, critically revised, and finalized the final manuscript.

Data availability statement

The original contributions presented in the study are included in the article/Supplementary Material. Further inquiries can be directed to the corresponding author.

Acknowledgments

We would like to thank Essay Star (https://essaystar.com/index.html) for providing linguistic assistance during the preparation of this manuscript

Funding

This study was funded by the National Key Research and Development Program of China (2020YFA0910200) and (2021YFD1800500).

Disclosure

The authors report no conflict of interest.

References

1. Lan Z, Bastos M, Menzies D (2016) Treatment of human disease due to *Mycobacterium bovis*: a systematic review. Eur Respir J 48:1500-1503. https://doi.org/10.1183/13993003.00629-2016
2. Scott C, Cavanaugh JS, Pratt R, Silk BJ, LoBue P, Moonan PK (2016) Treatment of human disease due to *Mycobacterium bovis*: a systematic review. Eur Respir J 48:1500-1503. https://doi.org/10.1183/13993003.00629-2016
3. Scott C, Cavanaugh JS, Pratt R, Silk BJ, LoBue P, Moonan PK (2016) Human Tuberculosis Caused by *Mycobacterium bovis* in the United States, 2006-2013. Clin Infect Dis 63:594-601. https://doi.org/ 10.1093/CID/ciw371
4. Maciuszek M, Klak K, Rydz L, Verburg-van Kemenade BML, Chadzinska M (2020) Cortisol Metabolism in Carp Macrophages: A Role for Macrophage-Derived Cortisol in M1/M2 Polarization. Int J Mol Sci 21:8954 .https://doi.org/ 10.3390/ijms21238954
5. Locati M, Curtale G, Mantovani A (2020) Diversity, Mechanisms, Significance of Macrophage Plasticity. Annu Rev Pathol 15:123-147. https://doi.org/ 10.1146/annual-pathmechdis-012418-012718
6. Wel MP, Kim BH, Park ES, Boyle KB, Nayak K, Lagrange B, Herod A, Henry T, Zilbauer M, Rohde J, MacMicking JD, Row F (2020) Guanylate-binding proteins convert cytosolic bacteria into caspase-4 signaling platforms. Nat Immunol 21:880-891. https://doi.org/ 10.1038/s41590-020-0697-2
7. Fisch D, Bo H, Clough B, Hornung V, Yamamoto M, Shenoy AR, Frickel EM (2019) Human GBP1 is a microbe-specific gatekeeper of macrophage apoptosis pyroptosis. Embo j 38:e100926. https://doi.org/ 10.15252/embj.2018100926
8. Honkala AT, Tailor D, Malhotra SV (2019) Guanylate-Binding Protein 1: An Emerging Target in Inflammation Cancer. Front Immunol 10: 3139. https://doi.org/ 10.3389/fimmu.2019.03139
9. Luque-Martin R, Angell DC, Kalxdorf M, Bernard S, Thompson W, Eberl HC, Ashby C, Freudenberg J, Sharp C, Van den Bossche J, de Jonge WJ, Rioja I, Piranha RK, Neele AE, Winther MPJ, Mer PK (2021) IFN-γ Drives Human Monocyte Differentiation into Highly Proinflammatory Macrophages That Resemble a Phenotype Relevant to Psoriasis. J Immunol 207:555-568. https://doi.org/ 10.4049/jimmunol.2001310
10. Zhang S, Chu C, Wu Z, Liu F, Xie J, Yang Y, Qiu H (2020) IFIH1 Contributes to M1 Macrophage Polarization in ARDS. Front Immunol 11: 580838. https://doi.org/ 10.3389/fimmu.2020.580838
11. Hall TJ, Vernimmen D, Browne JA, Mullen MP, Gordon SV, MacHugh DE, O'Doherty AM (2019) Alveolar Macrophage Chromatin Is Modified to Orchestrate Host Response to *Mycobacterium bovis* Infection. Front Genet 10:1386. https://doi.org/ 10.3389/fgene.2019.01386

12. Kim BH, Shenoy AR, Kumar P, Bradfield CJ, MacMicking JD (2012) IFN-inducible GTPases in host cell defense. Cell Host Microbe 12:432-44. https://doi.org/ 10.1016/j.chom.2012.09.007
13. Kim BH, Shenoy AR, Kumar P, Das R, Tiwari S, MacMicking JD (2011) A family of IFN-γ-inducible 65-kD GTPases protects against bacterial infection. Science 332:717-21. https://doi.org/ 10.1126/science.1201711
13. Maimon A, Levi-Yahid V, Ben-Meir K, Halpern A, Talmi Z, Priya S, Mizrahi G, Mistriel-Zerbib S, Berger M, Baniyash M, Loges S, Burstyn-Cohen T (2021) Myeloid cell-derived PROS1 inhibits tumor metastasis by regulating inflammatory immune responses via IL-10. J Clin Invest 131:e126089. https://doi.org/ 10.1172/jci126089
14. Qin Y, Wang Q, Zhou Y, Duan Y, Gao Q (2016) Inhibition of IFN-γ-Induced Nitric Oxide Dependent Antimycobacterial Activity by miR-155 C/EBPβ. Int J Mol Sci 17:535. https://doi.org/ 10.3390/ijms17040535
15. Rade MR, Amaral EP, Ribeiro SC, Almeida FM, Peres TV, Lanes V, D'Império-Lima MR, Lasunskaia EB (2012) Pathogenic *Mycobacterium bovis* strains differ in their ability to modulate the proinflammatory activation phenotype of macrophages. BMC Microbiol 12: 166. https://doi.org/ 10.1186/1471-2180-12-166
16. Rao V, Dhar N, Shakila H, Singh R, Khera A, Jain R, Naseema M, Paramasivan CN, Narayanan PR, Ramanathan VD, Tyagi AK (2005) Increased expression of *Mycobacterium tuberculosis* 19 kDa lipoprotein obliterates the protective efficacy of BCG by polarizing host immune responses to the Th2 subtype. Scand J Immunol 61:410-7. https://doi.org/ 10.1111/j.1365-3083.2005.01569.x
17. Tang J, Xu L, Zeng Y, Gong F (2021) Effect of gut microbiota on LPS-induced acute lung injury by regulating the TLR4/NF-kB signaling pathway. Int Immunopharmacol 91: 107272. https://doi.org/ 10.1016/j.intimp.2020.107272
18. Liu PT, Stenger S, Li H, Wenzel L, Tan BH, Krutzik SR, Ochoa MT, Schauber J, Wu K, Meinken C, Kamen DL, Wagner M, Bals R, Steinmeyer A, Zügel U, Gallo RL, Eisenberg D, Hewison M, Hollis BW, Adams JS, Bloom BR, Modlin RL (2006) Toll-like receptor triggering of a vitamin D-mediated human antimicrobial response. Science 311:1770-3. https://doi.org/ 10.1126/science.1123933
19. Kim HS, Shin TH, Yang SR, Seo MS, Kim DJ, Kang SK, Park JH, Kang KS (2010) The implication of NOD1 and NOD2 for the differentiation of multipotent mesenchymal stem cells derived from human umbilical cord blood. PLoS One 5: e15369. https://doi.org/ 10.1371/journal.pone.0015369
20. Liu Q, Tian Y, Zhao X, Jin H, Xie Q, Li P, Li D, Yan D, Zhu X (2015) NMAAP1 Expressed in BCG-Activated Macrophage Promotes M1 Macrophage Polarization. Mol Cells 38: 886-94. https://doi.org/ 10.14348/molcells.2015.0125
21. Gong Z, Han S, Liang T, Zhang H, Sun Q, Pan H, Wang H, Yang J, Cheng L, Lv X, Yue Q, Fan L, Xie J (2021) *Mycobacterium tuberculosis* effector PPE36 attenuates host cytokine storm damage via inhibiting macrophage M1 polarization. J Cell Physiol 236: 7405-7420. https://doi.org/ 10.1002/JCP.30411

22. Wang X, Chen S, Ren H, Chen J, Li J, Wang Y, Hua Y, Wang X, Huang N (2019) HMGN2 regulates non-tuberculous mycobacteria survival via modulation of M1 macrophage polarization. J Cell Mol Med 23: 7985-7998. https://doi.org/ 10.1111/jcmm.14599
23. Wang J, Liu Z, Li W, Yu J, Zhang D (2022) Knockdown of GBP1 inhibits BCG-induced apoptosis in macrophage RAW 264.7 cells via p38/JNK pathway. Infect Genet Evol 97: 105158. https://doi.org/ 10.1016/j.meegid.2021.105158
24. Santos JC, Boucher D, Schneider LK, Demarco B, Dilucca M, Shkarina K, Heilig R, Chen KW, Lim RYH, Broz P (2020) Human GBP1 binds LPS to initiate assembly of a caspase-4 activating platform on cytosolic bacteria. Nat Commun 11: 3276. https://doi.org/ 10.1038/s41467-020-16889-z
25. Lubeseder-Martellato C, Guenzi E, Jörg A, Töpolt K, Naschberger E, Kremmer E, Zietz C, Tschachler E, Hutzler P, Schwemmle M, Matzen K, Grimm T, Ensoli B, Stürzl M (2002) Guanylate-binding protein-1 expression is selectively induced by inflammatory cytokines is an activation marker of endothelial cells during inflammatory diseases. Am J Pathol 161: 1749-59. https://doi.org/ 10.1016/s0002-9440(10)64452-5
26. Guenzi E, Töpolt K, Cornali E, Lubeseder-Martellato C, Jörg A, Matzen K , Zietz C, Kremmer E, Nappi F, Schwemmle M, Hohenadl C, Barillari G, Tschachler E, Monini P, Ensoli B, Stürzl M (2001) The helical domain of GBP-1 mediates the inhibition of endothelial cell proliferation by inflammatory cytokines. Embo j 20: 5568-77. https://doi.org/ 10.1093/emboj/20.20.5568
27. Naschberger E, Wenzel J, Kretz CC, Herrmann M, Stürzl M, Kuhn A (2011) Increased expression of guanylate binding protein-1 in lesional skin of patients with cutaneous lupus erythematosus. Exp Dermatol 20:102-6. https://doi.org/ 10.1111/j.1600-0625.2010.01160.x
28. Fitzgerald KA, Kagan JC (2020) Toll-like Receptors the Control of Immunity. Cell 180:1044-1066. https://doi.org/ 10.1016/j.cell.2020.02.041
29. Kanehisa M, Goto S, Kawashima S, Okuno Y, Hattori M (2004) The KEGG resource for deciphering the genome. Nucleic Acids Res 32: D277-80. https://doi.org/ 10.1093/var/gkh063
30. Yi M, Horton JD, Cohen JC, Hobbs HH, Stephens RM (2006) WholePathwayScope: a comprehensive pathway-based analysis tool for high-throughput data. BMC Bioinformatics 7: 30. https://doi.org/ 10.1186/1471-2105-7-30

Tables

Table 1. The specific siRNA sequence in this study

Names	sense (5’-3’)	antisense (5’-3’)
siGBP2b-1	GCAGCACCUUCAUCUACAATT	UUGUAGAUGAAGGUGCUGCTT
siGBP2b-2	GACCAGCUGAAUAAAGAAUTT	AUUCUUUAUUCAGCUGGUCTT
siGBP2b-3	GAGCAACAAAGAAUCAUAUTT	AUAUGAUUCUUUGUUGCUCTT
siTLR4-1	GCUAUAGCUUCUCCAAUUUTT	AAAUUGGAGAAGCUAUAGCTT
siTLR4-2	GGACAGCUUAUAACCUUAATT	UUAAGGUUAUAAGCUGUCCTT
siTLR4-3	CCUCCAUAGACUUCAAUUATT	UAAUUGAAGUCUAUGGAGGTT
siCon	UUCUCCGAACGUGUCACGUTT	ACGUGACACGUUCGGAGAATT

Table 2. Primers for qRT-PCR in this study

Names	sense (5'-3')	antisense (5'-3')
iNOS	TGGTGAAGGGACTGAGCTGT	GCTACTCCGTGGAGTGAACA
TNF-a	TAGCCCACGTCGTAGCAAAC	GCAGCCTTGTCCCTTGAAGA
IL-1β	TGCCACCTTTTGACAGTGATG	TGATGTGCTGCTGCGAGATT
IL-6	CCCCAATTTCCAATGCTCTCC	CGCACTAGGTTTGCCGAGTA
Ccl5	TAGTCCTAGCCAGCTTGGGG	GAGCAGCTGAGATGCCCATT
Cxcl9	GATTGGTGCCCAGTTAGCCT	CCACCGGACAGCACTCTAAA
Ccr2	TTCTCAATTTCTCTGCGGCTG	AGTGGGGTCAGAGAAACACC
Lcn2	GGCCAGTTCACTCTGGGAAA	TGGCGAACTGGTTGTAGTCC
Cd40	GAGCCCTGTGATTTGGCTCT	AGATGGACCGCTGTCAACAA
Nos2	CTTGGTGAAGGGACTGAGCTG	TCCAAATCCAACGTTCTCCGT
Serpina3g	GCCTGAAAGAGAGCACATTG	CATTCGGGTCAAAGGGGTTC
Ccr2	GCCATCATAAAGGAGCCATACC	ATGCCGTGGATGAACTGAGG
Saa3	AACTATGATGCTGCCCGGAG	GCTCCATGTCCCGTGAACTT
Gbp2b	GAGTACTCTCTGGAA	TAGATGAAGGTGCTG
Iigp1	GGGGCAGGAGTGGATTTCATT	GCGTCCAGTGGATTCACACA
Il1a	ACGTCAAGCAACGGGAAGAT	AAGGTGCTGATCTGGGTTGG

Figures

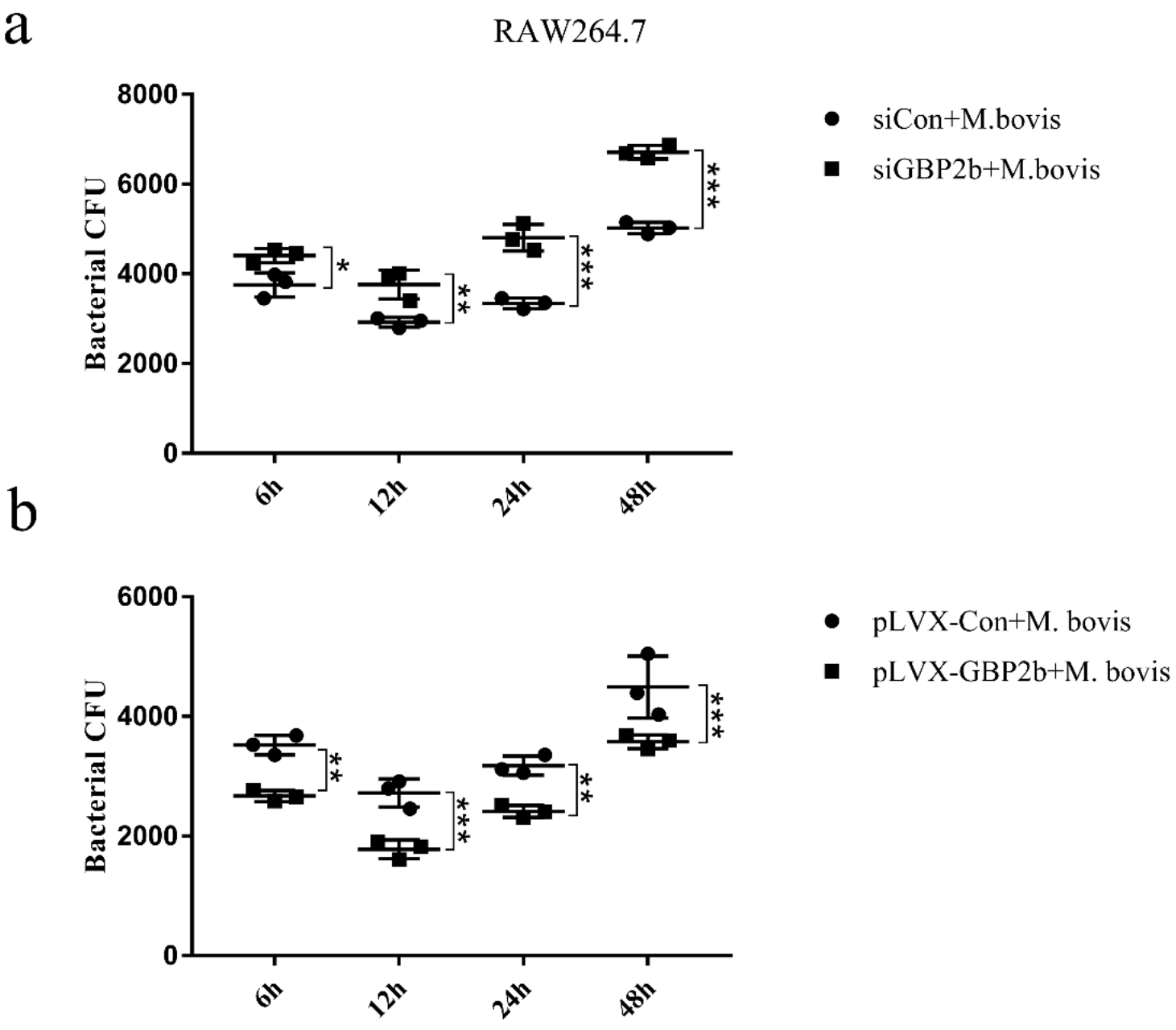

Figure 3

GBP2b regulates the balance of *M. bovis* replication in RAW264 cells.

(a) Colony-forming units (CFUs) in RAW264 cells at different time points (6, 12, and 24 h) after being transfected with siCon (nontargeted siRNA) or siGBP2b (GBP2b targeted siRNA) and infected with *M. bovis* (MOI 10) were calculated. (b) Colony-forming units (CFUs) in RAW264 cells at different time points (6, 12, and 24 h) after being transfected with pLVX-Con (control plasmid) or pLVX-GBP2b (GBP2b overexpression plasmid) and infected with *M. bovis* (MOI 10) were calculated. Data shown are means of

three independent experiments. Statistical difference was determined using a one-way analysis of variance test (ANOVA). *, $P < 0.05$; **, $P < 0.01$; ***, $P < 0.001$.

Figure 6

GBP2b promotes NO and ROS production during *M. bovis* infection.

(a) The NO release levels of RAW264.7 cells at different time points (0, 6, 12, and 24 h) after being transfected with siCon or siGBP2b and infected with *M. bovis* (MOI 10) were calculated by measuring the absorbance at 540 nm, respectively. (b) The NO release levels of RAW264.7 cells at different time points (0, 6, 12, and 24 h) after being transfected with pLVX-Con or pLVX-GBP2b and infected with *M. bovis* (MOI 10) were calculated by measuring the absorbance at 540 nm, respectively. (c) The ROS release levels of RAW264.7 cells at different time points (0, 6, 12, and 24 h) after being transfected with siCon or siGBP2b and infected with *M. bovis* (MOI 10) were detected by flow cytometry, respectively. (d) The ROS release levels of RAW264.7 cells at different time points (0, 6, 12, and 24 h) after being transfected with pLVX-Con or pLVX-GBP2b and infected with *M. bovis* (MOI 10) were detected by flow cytometry, respectively. Data shown are means of three independent experiments. Statistical difference was determined using a one-way analysis of variance test (ANOVA). *, $P < 0.05$; **, $P < 0.01$; ***, $P < 0.001$; ns, no significance.

Supplementary Files

This is a list of supplementary files associated with this preprint. Click to download.

- TableS3.M0BMDMsInfecttionVsM0BMDMsUninfectiondifferentialmRNA.pdf
- TableS6.mRNACoexpressionResult.pdf
- TableS8.Gbp2bComRNAPathwayregulatoryrelationship.pdf
- Onlinefloatimage10.png